

A quantum Monte Carlo algorithm for Bose-Hubbard models on arbitrary graphs

Emre Akaturk

Information Sciences Institute, University of Southern California, Marina del Rey, California 90292, USA

Itay Hen

Information Sciences Institute, University of Southern California, Marina del Rey, California 90292, USA and

*Department of Physics and Astronomy and Center for Quantum Information Science & Technology,
University of Southern California, Los Angeles, California 90089, USA**

We propose a quantum Monte Carlo algorithm capable of simulating the Bose-Hubbard model on arbitrary graphs, obviating the need for devising lattice-specific updates for different input graphs. We show that with our method, which is based on the recently introduced Permutation Matrix Representation Quantum Monte Carlo [Gupta, Albash and Hen, *J. Stat. Mech.* (2020) 073105], the problem of adapting the simulation to a given geometry amounts to generating a cycle basis for the graph on which the model is defined, a procedure that can be carried out efficiently and in an automated manner. To showcase the versatility of our approach, we provide simulation results for Bose-Hubbard models defined on two-dimensional lattices as well as on a number of random graphs.

I. INTRODUCTION

The Bose-Hubbard (BH) model, one of the pillars of condensed matter physics, is the go-to model for a large variety of physical phenomena, from Mott-Insulator-to-superfluid transitions to bosonic atoms in optical lattices. Similar to many other fundamental quantum systems of importance in condensed matter physics, the BH model does not admit analytical solutions in the general case and studying it usually requires resorting to approximation techniques, as even exact-numerical methods become unfeasible with increasing system size.

The most common approach for studying the BH model is statistical Quantum Monte Carlo (QMC) techniques [1–4]. QMC has been used to study the BH model throughout the years in a variety of contexts. Among these are supersolid phases [5–12], superfluid to Mott insulator transition [13–17] and superfluid to Bose glass transitions [13, 15, 18, 19]. Other studies focus on the BH model manifested on optical lattices with confining potentials [20–23] and extensions thereof [7, 11, 12, 24, 25].

Different setups of the BH model varying in both dimension and geometry have been explored, most notably with the Stochastic Series Expansion technique [26–29], employing different types of updates including dual vortex theory [30], multi-site generalization [31] or directed loops [11]. Other examples include studying the model on one-dimensional lattices [19, 25, 32–36], triangular [8–11, 16] or rectangular lattices in two dimensions [5–7, 12–15, 17, 37–41] and cubic lattices in three dimensions [20, 42, 43]. Other lattice types include a cubic lattice with a harmonic confining potential [44], the kagome lattice [30], the star lattice [31], the honeycomb lattice [24] and more [45].

One notable observation from the above survey is that simulating the BH model on different lattice structures

and in different dimensions with QMC often requires one to concoct specially tailored QMC updates for each such setup. In this study, we present a resolution to this obstacle by proposing a quantum Monte Carlo simulation technique that is applicable to Bose-Hubbard models defined on arbitrary input graphs, obviating the need for implementing lattice-specific update rules for each setup separately. The proposed technique may be used to simulate the BH model on any graph and in any dimension (for the first time, as far as the authors are aware).

Our approach builds on the parameter-free Trotter error-free Permutation Matrix Representation (PMR) quantum Monte Carlo technique introduced in Ref. [46] for spin systems, wherein the quantum partition function is expanded in a power series of the off-diagonal strength of the Hamiltonian, augmented with the necessary modifications that allow simulations of the Bose-Hubbard model on arbitrary graphs. Specifically, we show that QMC updates guaranteeing ergodicity and which also maintain detailed balance can be achieved by generating what is known as a minimal cycle basis on the BH graph [47] – the set of cycles that form a basis for all cycles on the graph [48]. We validate our proposed algorithm by simulating the Bose-Hubbard model on regular lattices as well as on a number of irregular graphs with up to 64 sites and with varying numbers of particles and Hamiltonian parameters to showcase the capabilities of our technique.

The paper is structured as follows: In Sec. II, we provide an overview of the PMR quantum Monte Carlo technique, followed by the specifics of our proposed QMC algorithm adapted to simulating BH models on arbitrary graphs. We then explain the concept of minimal cycle basis and its usage in the generation of the QMC updates for the algorithm in Sec. III. In Sec. IV, we present some simulation results for a number of Bose-Hubbard models defined on a variety of graphs. We summarize our work in Sec. V along with some conclusions and a discussion of future work.

* itayhen@isi.edu

II. THE QMC ALGORITHM

Our proposed QMC algorithm builds on the recently introduced Permutation Matrix Representation QMC (PMR-QMC) method [46]. Below we provide a brief overview of the general methodology, which we then discuss in more detail in the context of the Bose-Hubbard model.

A. Permutation matrix representation

The basis for the PMR-QMC method begins with casting the to-be-simulated Hamiltonian H in PMR form, namely, as

$$H = \sum_{j=0}^M \tilde{P}_j = \sum_{j=0}^M D_j P_j = D_0 + \sum_{j=1}^M D_j P_j, \quad (1)$$

where $\{\tilde{P}_j\}_{j=0}^M$ is a set of $M+1$ distinct generalized permutation matrices [49] – matrices that have at most one nonzero element in each row and each column. One can write each \tilde{P}_j as $\tilde{P}_j = D_j P_j$ where D_j is a diagonal matrix and P_j is a bona fide permutation matrix. One of the permutations, which we denote by P_0 , can always be chosen to be $P_0 = \mathbb{1}$ (the identity operation), such that the other permutation matrices have no fixed points, i.e., no nonzero diagonal elements. We refer to the basis in which the $\{D_j\}$ matrices are diagonal as the computational basis and denote its states by $\{|z\rangle\}$. The operators $D_j P_j$ for $j > 0$ represent the ‘quantum dimension’ of the Hamiltonian. Acting with a $D_j P_j$ matrix on a basis state $|z\rangle$ gives $D_j P_j |z\rangle = d_j(z')|z'\rangle$ where $d_j(z')$ is a (generally complex) coefficient and $|z'\rangle$ is a basis state $|z\rangle \neq |z'\rangle$. We will refer to D_0 (the matrix multiplying P_0) as the ‘classical Hamiltonian’. The permutation matrices derived from H are a subset of the permutation group wherein P_0 is the identity element [46]. One can show that any finite-dimensional (or countable infinite-dimensional) matrix can be written in PMR form [46].

B. The off-diagonal partition function expansion

Having cast the Hamiltonian in PMR form, one proceeds with expanding the canonical partition function $Z = \text{Tr}[e^{-\beta H}]$ about its diagonal part in powers of its off-diagonal strength [46]. The expansion results in the following expression for the partition function (a detailed derivation can be found in Appendix A and in Ref. [46]).

$$Z = \sum_z \sum_{S_{i_q}=\mathbb{1}} D_{(z, S_{i_q})} e^{-\beta [E_{z_0}, \dots, E_{z_q}]} \quad (2)$$

The double sum above runs over all computational basis states $|z\rangle$ and all products $S_{i_q} = P_{i_q} \dots P_{i_2} P_{i_1}$ of permutation operators that evaluate to the identity. Here

$q = 0, \dots, \infty$ denotes the number of elements in each product. Specifically, $\mathbf{i}_q = (i_1, i_2, \dots, i_q)$ is a q -element multi-index where each index i_j ($j = 1 \dots q$) runs from 1 to M .

In the above sum, each summand is a product of two terms. The first is $D_{(z, S_{i_q})} \equiv \prod_{j=1}^q d_{z_j}^{(i_j)}$ consisting of a product of the matrix elements

$$d_{z_j}^{(i_j)} = \langle z_j | D_{i_j} | z_j \rangle. \quad (3)$$

The various $\{|z_j\rangle\}$ states are the states obtained from the action of the ordered P_j operators in the product S_{i_q} on $|z_0\rangle$, then on $|z_1\rangle$, and so forth. For example, for $S_{i_q} = P_{i_q} \dots P_{i_2} P_{i_1}$, we obtain $|z_0\rangle = |z\rangle$, $P_{i_1}|z_0\rangle = |z_1\rangle$, $P_{i_2}|z_1\rangle = |z_2\rangle$, etc. The proper indexing of the states $|z_j\rangle$ along the path is $|z_{(i_1, i_2, \dots, i_j)}\rangle$ to indicate that the state in the j -th step depends on all $P_{i_1} \dots P_{i_j}$. For conciseness, we will use the shorthand $|z_j\rangle$. The sequence of basis states $\{|z_j\rangle\}$ may be viewed as a closed ‘walk’ on the Hamiltonian graph – the graph defined by H such that the H_{ij} matrix element corresponds to an edge between the two basis states i and j , which serve as nodes on the graph.

The second term in each summand, $e^{-\beta [E_{z_0}, \dots, E_{z_q}]}$, is called the divided differences of the function $F(\cdot) = e^{-\beta(\cdot)}$ with respect to the inputs $[E_{z_0}, \dots, E_{z_q}]$. The divided differences [50, 51] of a function $F(\cdot)$ is defined as,

$$F[E_{z_0}, \dots, E_{z_q}] \equiv \sum_{j=0}^q \frac{F(E_{z_j})}{\prod_{k \neq j} (E_{z_j} - E_{z_k})}. \quad (4)$$

In our case, the inputs E_{z_j} are defined as $E_{z_j} = \langle z_j | D_0 | z_j \rangle$. The reader is referred to Appendix A for additional details.

C. PMR of the Bose-Hubbard model

The Bose-Hubbard Hamiltonian, which is the focus of this study, is given by

$$H = -t \sum_{m=1}^M \hat{b}_{j_m}^\dagger \hat{b}_{k_m} + \frac{U}{2} \sum_{i=1}^L \hat{n}_i (\hat{n}_i - 1) - \mu \sum_{i=1}^L \hat{n}_i, \quad (5)$$

where in the above expression $i = 1, \dots, L$ labels the sites, which we will treat as graph nodes for reasons that will become clear later, and $m = 1, \dots, M$ labels the (directed) ‘edges’ of the model, i.e., the ordered pairs of sites (j_m, k_m) between which hopping terms $\hat{b}_{j_m}^\dagger \hat{b}_{k_m}$ exist. In addition, hermiticity of the Hamiltonian dictates that for every pair of indices (j_m, k_m) there exists another pair $(j_{m'}, k_{m'})$ such as $(j_{m'}, k_{m'}) = (k_m, j_m)$, corresponding to a hopping term in the opposite direction.

As the computational basis for the PMR expansion, we use the second quantized occupation number basis for bosons, where a basis state is given as $|\mathbf{n}\rangle = |n_1, n_2, \dots, n_L\rangle$ with L being the number of sites

and n_1, \dots, n_L are nonnegative integers representing the number of bosons in each site. We denote the total number of bosons, $\sum_{i=1}^L n_i$, by N . The operators $\hat{b}_i^\dagger, \hat{b}_i$ are creation and annihilation operators, respectively, obeying

$$\hat{b}_i^\dagger \hat{b}_j |\mathbf{n}\rangle = \sqrt{(n_i + 1)n_j} |\mathbf{n}^{(i,j)}\rangle, \quad (6)$$

where $|\mathbf{n}^{(i,j)}\rangle$ stands for the state $|\mathbf{n}\rangle$ with one additional boson at site i and one fewer at site j . The operator $\hat{n}_i = \hat{b}_i^\dagger \hat{b}_i$ is the number operator. The coefficients t, U and μ are real-valued parameters.

Casting H in PMR form with respect to the second quantized basis dictates that the diagonal term D_0 consists of the on-site terms, namely,

$$D_0 = \frac{U}{2} \sum_i \hat{n}_i (\hat{n}_i - 1) - \mu \sum_i \hat{n}_i. \quad (7)$$

Likewise, the generalized permutation operators of the BH model are $\tilde{P}_m = -t \hat{b}_{j_m}^\dagger \hat{b}_{k_m}$. These can be written as products of bonafide permutation operators which obey

$$P_m |\mathbf{n}\rangle = |\mathbf{n}^{(j_m, k_m)}\rangle, \quad (8)$$

and accompanying diagonal operators

$$D_m = -t \sum_{\mathbf{n}} \sqrt{n_{j_m} (n_{k_m} + 1)} |\mathbf{n}\rangle \langle \mathbf{n}|, \quad (9)$$

which together give $\tilde{P}_m = D_m P_m$. Here, the summation index \mathbf{n} runs over all basis states (though due to conservation of number of particles, the sum of over states \mathbf{n} can be restricted to those states that obey $\sum_{i=1}^L n_i = N$). The total Hamiltonian can now be recast as

$$H = D_0 + \sum_{m=1}^M D_m P_m. \quad (10)$$

Using the above notation, the partition function can be written as

$$Z = \sum_{\mathbf{n}} \sum_{\mathbf{i}_q} W_{(\mathbf{n}, \mathbf{i}_q)} = \sum_{\mathbf{n}} \sum_{\mathbf{i}_q} D_{(\mathbf{n}, \mathbf{i}_q)} e^{-\beta [E_{\mathbf{n}_0}, \dots, E_{\mathbf{n}_q}]} \quad (11)$$

As already discussed, the operator sequences are of the form $S_{\mathbf{i}_q} = P_{i_q} \dots P_{i_2} P_{i_1}$ and must evaluate to the identity operation. Each $S_{\mathbf{i}_q}$ generates a sequence of states $|\mathbf{n}_0\rangle = |\mathbf{n}\rangle, P_{i_1} |\mathbf{n}_0\rangle = |\mathbf{n}_1\rangle, P_{i_2} |\mathbf{n}_1\rangle = |\mathbf{n}_2\rangle$ and so on where the last state is $|\mathbf{n}_q\rangle = |\mathbf{n}_0\rangle$. Moreover,

$$D_{(\mathbf{n}, \mathbf{i}_q)} = \prod_{r=1}^q d_{\mathbf{n}_r}^{(i_r)}, \text{ where}$$

$$d_{\mathbf{n}_r}^{(m)} = \langle \mathbf{n}_r | D_m | \mathbf{n}_r \rangle = -t \sqrt{n_{j_m}^{(r)} (n_{k_m}^{(r)} + 1)}. \quad (12)$$

Here, $n_i^{(r)}$ refers to the i -th element of the state $|\mathbf{n}_r\rangle$.

D. The algorithm

1. Preliminaries

Having presented the partition function as a sum of efficiently computable terms [Eq. (11)], we can now devise a QMC algorithm, i.e., a Markov chain Monte Carlo process, based on this decomposition. The partition function has the form of a sum configuration weights

$$Z = \sum_{\mathcal{C}} W_{\mathcal{C}}, \quad (13)$$

where the weights are given by

$$W_{\mathcal{C}} = D_{(\mathbf{n}, \mathbf{i}_q)} e^{-\beta [E_{\mathbf{n}_0}, \dots, E_{\mathbf{n}_q}]}, \quad (14)$$

and each configuration \mathcal{C} is the pair $\mathcal{C} = \{|\mathbf{n}\rangle, S_{\mathbf{i}_q}\}$. Here, $|\mathbf{n}\rangle$ is the basis state of the configuration and $S_{\mathbf{i}_q}$ is a product of operators that evaluates to $\mathbb{1}$. As already discussed, each configuration \mathcal{C} induces a closed walk on the Hamiltonian graph, a sequence of states $|\mathbf{n}\rangle = |\mathbf{n}_0\rangle, |\mathbf{n}_1\rangle, \dots, |\mathbf{n}_q\rangle = |\mathbf{n}\rangle$ which is acquired by acting with the permutation operators in $S_{\mathbf{i}_q}$, in sequence, on $|\mathbf{n}\rangle$.

2. The initial configuration

The initial configuration of our QMC algorithm is set to be $\mathcal{C}_0 = \{|\mathbf{n}\rangle, S_0 = \mathbb{1}\}$, where $|\mathbf{n}\rangle$ is a randomly chosen basis state acquired by acting with a predetermined number of randomly picked operators P_i on a predetermined basis state $|\mathbf{n}\rangle$, which we choose to be $|\mathbf{n}\rangle = |N, 0, 0, \dots, 0\rangle$ (recall that N is the total number of particles). The sequence of permutation operators is simply the empty sequence, for which $q = 0$. The weight of the initial state is therefore given by $W_{\mathcal{C}_0} = e^{-\beta [E_{\mathbf{n}}]} = e^{-\beta E_{\mathbf{n}}}$.

3. The QMC updates

To ensure that every configuration in configuration space is reachable from any other, i.e., that the Markov chain is ergodic, we utilize five different types of moves. These are (i) ‘classical’ moves, (ii) local swap moves (iii) cyclic rotation moves, (iv) block swaps and (v) insertion-deletion moves. We discuss these in detail below. We then show that this set of moves together is sufficient to guarantee ergodicity.

Classical moves.— Classical moves ensure that all basis states $|\mathbf{n}\rangle$ can be reached. During this move, a new basis state $|\mathbf{n}'\rangle$ is proposed to replace the current one $|\mathbf{n}\rangle$ in the configuration \mathcal{C} . The sequence of operators $S_{\mathbf{i}_q}$ is not altered. The new basis state is chosen by acting with a randomly selected operator P_m on the current basis state. In the case where the proposed new state $|\mathbf{n}'\rangle$ is

not a valid state, i.e., whenever $P_m|\mathbf{n}\rangle = 0$, the procedure is repeated until a valid state is produced. The new configuration is accepted with probability $\min(1, W_{\mathcal{C}'} / W_{\mathcal{C}})$ where $W_{\mathcal{C}'}$ is the weight of the proposed configuration \mathcal{C}' and $W_{\mathcal{C}}$ is the weight of the current one \mathcal{C} .

Local swap moves.— A local swap move consists of randomly picking two adjacent operators in $S_{\mathbf{i}_q}$ and then swapping them to create a new sequence $S'_{\mathbf{i}_q}$. Here too, the new configuration is accepted with probability $\min(1, W_{\mathcal{C}'} / W_{\mathcal{C}})$ where $W_{\mathcal{C}'}$ is the weight of the proposed configuration \mathcal{C}' and $W_{\mathcal{C}}$ is the weight of the current one \mathcal{C} .

Cyclic rotation moves.— The cyclic rotation move consists of rotating (typically small length) sub-sequences within $S_{\mathbf{i}_q}$ that evaluate to $\mathbb{1}$ – we shall refer to these as cycles – utilizing the fact that a rotated sub-sequence that evaluates to $\mathbb{1}$ also evaluates to $\mathbb{1}$. The chosen sub-sequence S is virtually ‘cut’ to two so that it can be written as $S = S_1 S_2$. Then, S is replaced with the modified sub-sequence $S' = S_2 S_1$ in $S_{\mathbf{i}_q}$. Here too, the new configuration is accepted with probability $\min(1, W_{\mathcal{C}'} / W_{\mathcal{C}})$ where $W_{\mathcal{C}'}$ is the weight of the proposed configuration \mathcal{C}' and $W_{\mathcal{C}}$ is the weight of the current one \mathcal{C} .

Block swap moves.— The block swap move modifies both the basis state and the sequence of operators. Here, a random position k in the product $S_{\mathbf{i}_q}$ is picked such that the product is split into two (non-empty) sub-sequences, $S_{\mathbf{i}_q} = S_2 S_1$, with $S_1 = P_{i_k} \cdots P_{i_1}$ and $S_2 = P_{i_q} \cdots P_{i_{k+1}}$. Denoting the classical state at position k in the product as $|\mathbf{n}'\rangle$, namely,

$$|\mathbf{n}'\rangle = S_1 |z\rangle = P_{i_k} \cdots P_{i_1} |\mathbf{n}\rangle, \quad (15)$$

where $|\mathbf{n}\rangle$ is the classical state of the current configuration, the new block-swapped configuration is $\mathcal{C}' = \{|\mathbf{n}'\rangle, S_1 S_2\}$.

Insertion-deletion moves.— The insertion-deletion move is the only type of move considered here that changes the length q of the sequence of operators. An insertion-deletion move either removes cycles (sequences of operators that evaluates to the $\mathbb{1}$) from $S_{\mathbf{i}_q}$ or inserts a randomly picked cycle from a pool of ‘fundamental cycles’ (which we discuss in detail in the next section).

The insertion-deletion move consists of first randomly selecting a length m_l for the cycle that is to be inserted or removed among all possible cycle lengths. As the next step, a random choice is made as to whether insert a cycle or remove one from $S_{\mathbf{i}_q}$.

If deletion is selected, and $m_l = 2$, a uniformly random deletion point k is selected. If $P_{i_{k-1}} P_{i_k}$ is a cycle, i.e., evaluates to the identity operation, then a configuration with the two operators removed is proposed. Otherwise, the move is rejected. For $m_l > 2$, a deletion point k is selected in a similar manner. If $\{P_{i_{k-2}}, P_{i_{k-1}}, \dots, P_{i_{k+m_l-3}}\}$ is equivalent to $\mathbb{1}$ and the sequence is in the list of fundamental cycles, the sub-sequence is removed and the resultant configuration is proposed. Otherwise, no new configuration is proposed and the move is rejected.

If insertion is selected, a random insertion point k is selected. A random cycle of length m_l is picked from the pool of cycles which is then inserted into the full sequence $S_{\mathbf{i}_q}$ at position k . The proposed new configuration is then accepted or rejected based on its relative weight (and other selection factors) maintaining detailed balance.

Cycle completion.— Although not strictly necessary for ergodicity, one may augment the aforementioned QMC updates with another type of moves, which we refer to here as ‘cycle completion moves’. Here, one chooses a sub-sequence S_1 from $S_{\mathbf{i}_q}$ and subsequently checks whether S_1 is a sub-cycle of one the aforementioned fundamental cycles, namely if a fundamental cycle of the form $S_1 S_2 = \mathbb{1}$ exists. If it does, then S_1 is replaced (with the appropriate acceptance probability) with S_2^{-1} as both S_1 and its replacement evaluate to the same permutation.

E. Measurements

Deriving expressions for measurements of expectation values of essentially any physical observable is straightforward with PMR [52]. In this study we focus on measuring the thermal average of the diagonal, off-diagonal and total energies. One can calculate the average energy $\langle H \rangle$ using the expression:

$$\langle H \rangle = \frac{\text{Tr}[He^{-\beta H}]}{\text{Tr}[e^{-\beta H}]} = \frac{\sum_{(z,\mathbf{i})} W_{(z,\mathbf{i})} \left(E_z + \frac{e^{-\beta[E_{z_1}, \dots, E_{z_q}]}}{e^{-\beta[E_z, \dots, E_{z_q}]}} \right)}{\sum_{(z,\mathbf{i})} W_{(z,\mathbf{i})}}. \quad (16)$$

In the above expression we identify E_z as the instantaneous quantity that needs to be calculated for the diagonal energy throughout the simulation, namely,

$$\langle H_d \rangle = \frac{\text{Tr}[He^{-\beta H}]}{\text{Tr}[e^{-\beta H}]} = \frac{\sum_{(z,\mathbf{i})} W_{(z,\mathbf{i})} E_z}{\sum_{(z,\mathbf{i})} W_{(z,\mathbf{i})}}, \quad (17)$$

and $\frac{e^{-\beta[E_{z_1}, \dots, E_{z_q}]}}{e^{-\beta[E_z, \dots, E_{z_q}]}}$ as the corresponding quantity for the off-diagonal energy, that is:

$$\langle H_{od} \rangle = \frac{\text{Tr}[He^{-\beta H}]}{\text{Tr}[e^{-\beta H}]} = \frac{\sum_{(z,\mathbf{i})} W_{(z,\mathbf{i})} \frac{e^{-\beta[E_{z_1}, \dots, E_{z_q}]}}{e^{-\beta[E_z, \dots, E_{z_q}]}}}{\sum_{(z,\mathbf{i})} W_{(z,\mathbf{i})}}. \quad (18)$$

The sum of these two instantaneous quantities yields the instantaneous total energy.

Since the configurations are visited in proportion to their weights, a simple average of the above quantities will yield the correct expectation values for the diagonal, off-diagonal and total energies respectively. For other observables, which can similarly be sampled, the reader is referred to Ref. [52].

III. ERGODICITY AND MINIMAL CYCLE BASES

The QMC update moves used throughout the simulation must be able to generate an ergodic Markov chain for any input graph and dimensionality of the BH model. That is, any valid configuration $(|n\rangle, S_{i_q})$ has to be reachable from any other. While the various (second-quantized) basis states $|n\rangle$ are trivially reachable from one another by the so-called ‘classical moves’ discussed in the previous section, which randomly alter the basis states (augmented by block swap moves, which also change the basis state), less obvious is the guarantee that all operator sequences S_{i_q} evaluating to the identity are reachable from one another.

To show that the moves discussed in the previous section do indeed generate an ergodic Markov chain, we begin by making a few observations. The first is that local swap and cyclic rotation moves shuffle, or permute, the operators in the sequence of operators. Thus, to demonstrate ergodicity one only needs to show that all valid multi-sets of operators (irrespective of their ordering) are producible.

The second observation we make is that every permutation operator P_m in the BH model, which as already mentioned can be associated with a directed edge on the BH graph, has an inverse permutation $P_{m'}$ such that $P_{m'} = P_m^{-1}$ – the permutation operator associated with the same edge but which points in the opposite direction. The insertion-deletion move consisting of the insertion or deletion of pairs of operators $P_m P_m^{-1}$ therefore corresponds to the insertion and deletion of operators corresponding to the same edge (but with opposite directions) twice. The insertion-deletion of pairs can therefore be used to remove edge pairs down to a core collection of operators that multiply to the identity and in which operators do not appear with their inverses. We conclude then, that to guarantee ergodicity, the only remaining requirement is that there is an update move capable of generating all multi-sets of operators (whose product evaluates to the identity) which contain edges pointing only in one direction but never both (that is, sequences that never contain both P_m and P_m^{-1}). We shall call such multi-sets of operators ‘multi-cycles’. We shall call a multi-cycle that does not contain repeated edges a ‘cycle’ and note that any multi-cycle is a concentration of bona fide cycles.

In terms of edges on the BH graph, the ability to produce all multi-cycles reduces to the requirement that all cycles on the underlying BH graph can be produced, or inserted. An illustrative example of a single cycle on a BH graph is given in Fig. 1.

In what follows, we show that any cycle on a given BH graph can be produced via combinations of insertions and deletions of cycles taken from a finite set of cycles, commonly referred to as a cycle basis – a set of cycles that combinations thereof are capable of producing all possible cycles [47]. Setting up a QMC update

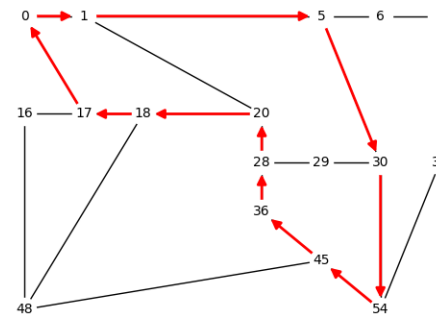


FIG. 1. An example of a random graph on which the BH model can be defined. Nodes correspond to sites that the bosons can occupy and every edge is associated with two permutation operators, or hopping terms – one in each direction. In red is an example of a set of (directed) edges whose corresponding sequence of operators multiply to the identity operation.

rule within which these ‘fundamental’ cycles are inserted or deleted (see Sec. II D 3) will ensure then that all cycles are producible, guaranteeing ergodicity as desired. We next discuss the process of generating a cycle basis for any given input graph.

Let us consider a K -edge BH graph. The $M = 2K$ permutation operators of the BH graph correspond to the directed edges, equivalently ordered pairs of nodes of the form (j_m, k_m) , corresponding to the existence of a permutation operator P_m in the Hamiltonian which creates a boson at site j_m and annihilates one at site k_m . A cycle c (of length $|c|$) is a set of edges that can be ordered as a sequence $\{(i_1, i_2), (i_2, i_3), \dots, (i_{|c|}, i_1)\}$ where $|c|$ denotes the number of edges in c , with the restriction that if an edge is in c then its inverse cannot be in c . Succinctly, a cycle may be written as a sequence of nodes $i_1 \rightarrow i_2 \rightarrow \dots \rightarrow i_{|c|} \rightarrow i_1$.

With the above definitions, one can assign every permutation operator P_m corresponding to a directed edge (j_m, k_m) a ternary vector $\mathbf{b}_m = (b_1, b_2, \dots, b_n)$ such that $b_{j_m} = 1$ (a boson is created at site j_m), $b_{k_m} = -1$ (a boson is annihilated at site k_m) and all other entries are set to zero. The product of two permutation operators would correspond to the addition of two such vectors. A cycle c would be a linear combination of ternary vectors adding up to the zero vector, namely, $\sum_{i=1}^M c_i \mathbf{b}_i = \mathbf{0}$ where $c_i \in \{-1, 0, 1\}$.

Finding a basis of cycles with which one could produce any possible cycle corresponds to finding a set of ternary vectors of the form $\mathbf{c} = \{c_1, \dots, c_M\}$ that solve the homogenous set of equations $\mathbf{B}\mathbf{c} = \mathbf{0}$ where \mathbf{B} is the $M \times n$ matrix consisting of the M column vectors \mathbf{b}_i ($i = 1, \dots, M$). Expressed differently, finding a cycle basis can be accomplished via finding the nullspace of the above linear system, which can be done efficiently using Gaussian elimination. In Fig. 2, we provide an example of a cycle basis found for the graph depicted in Fig. 1. In

the figure, a non-directed cycle is depicted as a collection of red-colored edges.

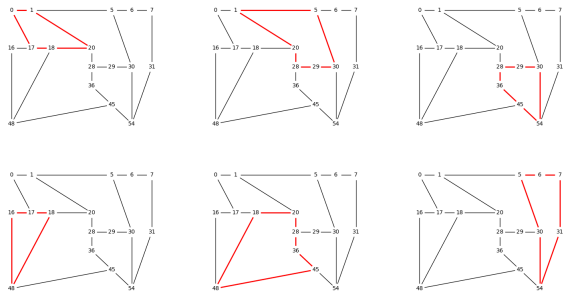


FIG. 2. A cycle basis for the graph depicted in Fig. 1. Every cycle on the BH graph can be represented as a combination (or a concatenation) of these basis cycles.

Denoting by T the dimension of the cycle nullspace, we note that the set of nullspace cycles is not unique, as any T linearly independent vectors may serve as a basis. For the QMC algorithm however, we find that in order to maximize the acceptance ratios of insertion and removal of cycles the length of cycles should preferably be as short as possible. We therefore devise a protocol for producing a minimal cycle basis [47, 53, 54] – the set of shortest possible cycles that form a basis. We find the minimal cycle basis using an algorithm proposed by Kavitha et al. [54].

We note that even though QMC updates based on the generation of a minimal cycle basis are sufficient to ensure an ergodic Markov chain, one may introduce additional cycles into the pool of ‘fundamental’ cycles to improve the convergence rate of the simulation. Having more cycles in the pool of cycles available to choose from will increase the acceptance rates of both the insertion-deletion and cycle completion updates. On the other hand, searching a long list of fundamental cycles stands to inevitably slow down the algorithm. We find that these two opposing considerations are appropriately balanced if one includes all the chordless cycles of the BH graph that have a length smaller than or equal to the longest basis cycle found (a chordless cycle is defined as a cycle that does not have a ‘chord’, i.e., a cycle for which there are no edges not belonging to the cycle that connect two vertices that do belong to it [48]).

IV. ALGORITHM TESTING

To test the power and flexibility of our method, we have carried out QMC simulations for a variety of BH models, implementing the algorithm introduced above allowing it to find within each setup a minimal cycle basis and in turn provably ergodic QMC updates. We next present the results of our simulations for several BH graph configurations including rectangular lattices with varying Hamiltonian parameters as well as irregular graphs.

A. Verification against exact diagonalization

To verify the correctness of our algorithm, we first carry out simulations of the BH model on small two-dimensional rectangular lattices so that the QMC results can be compared against those obtained from exact diagonalization.

For concreteness, we choose to monitor and measure the total energy, given in Eq. (16). It should be noted that our algorithm is readily capable of measuring many other physical observables as well [52]. All data points presented in this section were obtained via the execution of multiple independent simulations each of which yielding a single value for the total energy. Data points were obtained by averaging the values from each run whereas error bars were obtained by the evaluation of the sample error of the mean over said data points.

In Fig. 3(left), we plot the average thermal energy as a function of number of bosons N for a BH model on a 2×2 rectangular lattice (with open boundary conditions). The parameters for which results are shown are $t = 1, \mu = 0, U = 0.5$ and $\beta = 1$. Figure 3(middle) shows the average energy as a function of the on-site repulsion U for $N = 8$ bosons. Here, $t = 1, \mu = 1$ and $\beta = 1$. Another set of results for simulations of a 2×2 rectangular lattice with open boundary conditions is presented in Fig. 3(right). Here too, $N = 8$ and the average thermal energy is plotted as a function of inverse-temperature β (with $t = 1, \mu = 1$ and $U = 1$). As can be seen from the three panels of the figure, the QMC results are in excellent agreement with those obtained from exact diagonalization.

B. Larger two-dimensional lattices

Having verified the validity of our approach, we next provide simulation results for larger rectangular systems. Figure 4(top) depicts the average thermal energy as a function of the on-site repulsion U for a BH model defined on an 8×8 rectangular lattice with open boundary conditions containing $N = 64$ particles. The average thermal energy is plotted as a function of on-site potential U for a 6×6 rectangular lattice with periodic boundary conditions in Fig. 4(bottom). Here, $t = 1, \mu = 1$ and $\beta = 1$.

C. Simulations of the BH model on random graphs

To showcase the versatility of our approach we have also carried out QMC simulations of BH models defined on randomly generated graphs. For the results below, we present the graphs themselves and their fundamental basis cycles alongside the simulation results.

Starting with the 6-node random graph depicted in Fig. 5(left) alongside its minimal cycle basis, we present

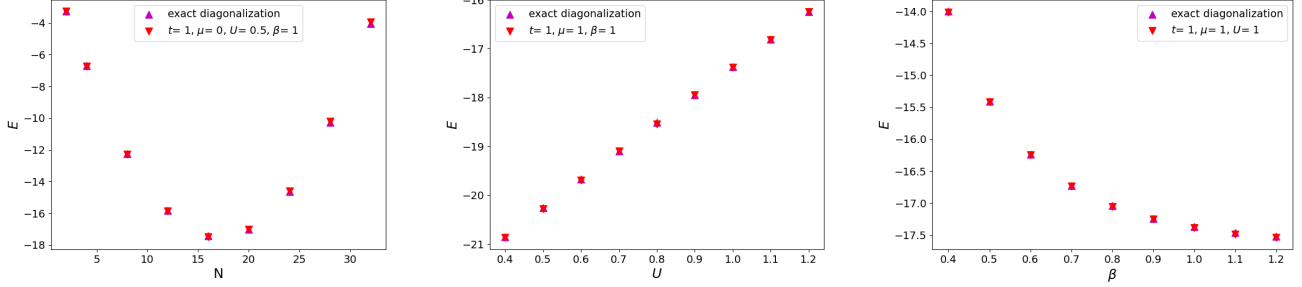


FIG. 3. Comparison of QMC results with exact diagonalization. Left: Average energy $E = \langle H \rangle$ as a function of total number of particles N for a 2 by 2 rectangular lattice with open boundary conditions and parameters $t = 1, \mu = 0, U = 0.5, \beta = 1$. Middle: Average energy $\langle H \rangle$ for a 2 by 2 rectangular lattice with $N = 8$ particles (open boundary conditions) and parameters $t = 1, \mu = 1, \beta = 1$ as a function of U . Right: Average energy for a 2 by 2 rectangular lattice with $N = 8$ particles (open boundary conditions) and parameters $t = 1, \mu = 1, U = 1$ as a function of inverse temperature β .

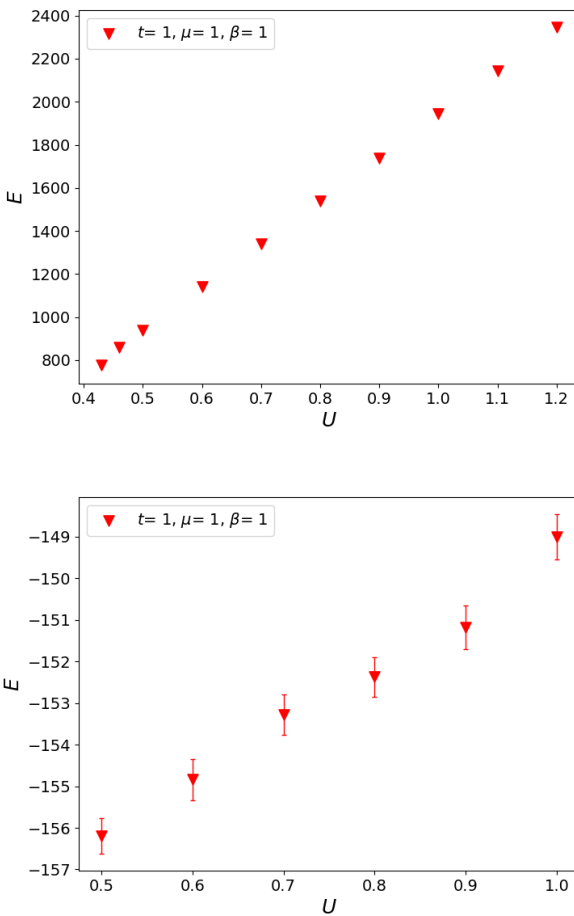


FIG. 4. Top: Average energy $E = \langle H \rangle$ for a BH model defined on an 8×8 rectangular lattice with open boundary conditions and $N = 64$ particles as a function of on-site potential U . Here, $t = 1, \mu = 1$ and $\beta = 1$. Bottom: Average energy $E = \langle H \rangle$ as a function of U for a 6×6 rectangular lattice with periodic boundary conditions and 36 particles. Here too, $t = 1, \mu = 1$ and $\beta = 1$.

the average energy of an $N = 6$ -boson system in Fig. 5(right) as a function of the on-site repulsion U .

In Fig. 6(right), we show results of simulations conducted on the 17-site graph shown in Fig. 6(left). Here, we measure the total energy of the system as a function of U for an $N = 17$ -boson system.

V. SUMMARY AND CONCLUSIONS

We presented a quantum Monte Carlo algorithm designed to reliably simulate the Bose-Hubbard model on arbitrary graphs. We showed that a provably ergodic QMC algorithm can be devised by adapting the Permutation Matrix Representation QMC [46] augmenting it with update moves based on the minimal cycle basis of the BH graph, which can be produced in an automated way.

To demonstrate the versatility and generality of our approach, we presented simulation results for the Bose-Hubbard model defined on regular lattices with open and periodic boundary conditions as well as on a number of irregular graphs.

We believe that the algorithm presented in this study may become a very useful tool in the study of the equilibrium properties of Bose-Hubbard models in different dimensions and setups, which have so far not been amenable to simulations.

Moreover, the methods presented in this paper are readily generalizable to other types of systems, e.g., fermionic or spin systems. We aim to explore such extended techniques in future work.

ACKNOWLEDGMENTS

This project was supported in part by NSF award #2210374. In addition, this material is based upon work supported by the Defense Advanced Research Projects Agency (DARPA) under Contract No. HR001122C0063.

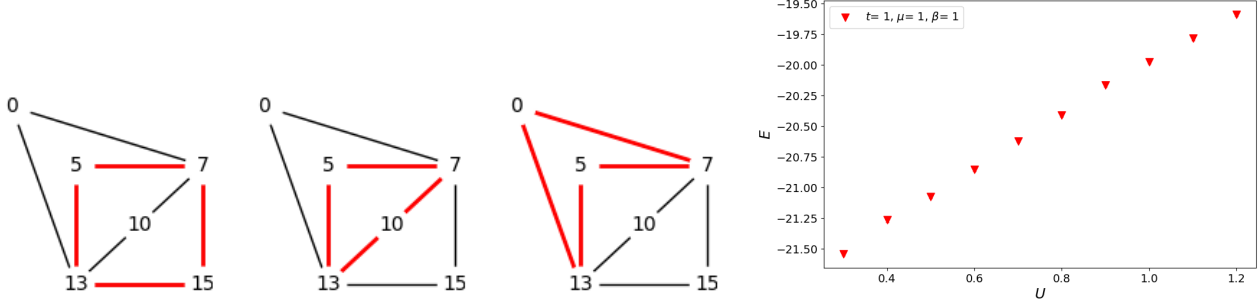


FIG. 5. Left: The minimal cycle basis (in red) for a six-node graph containing eight edges. Right: Average energy $E = \langle H \rangle$ as a function of U for the graph depicted in the left panel. Here, the number of particles is $N = 6$. The remaining parameters are fixed and have the following values: $t = 1, \mu = 1$ and $\beta = 1$.

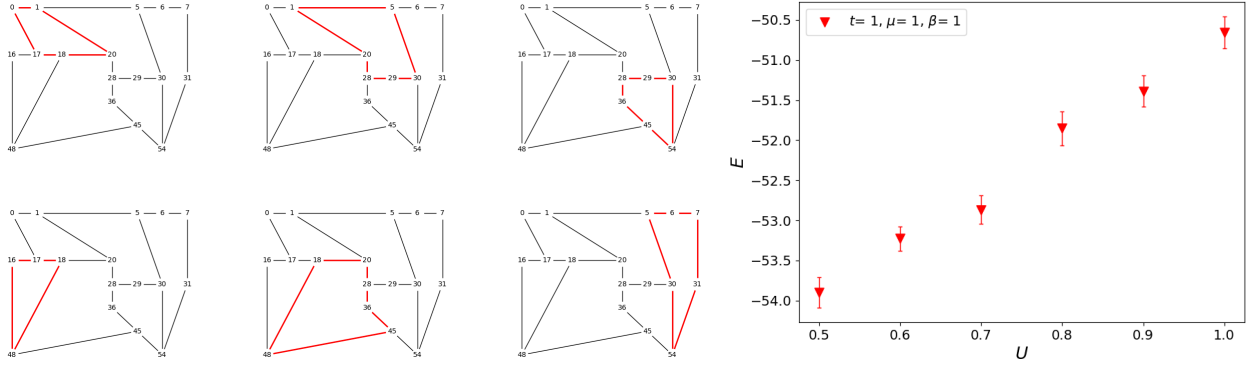


FIG. 6. Left: The minimal cycle basis (in red) for a 17-node random graph. Right: Average energy $E = \langle H \rangle$ as a function of U for the graph depicted in the left panel. Here, the number of particles is $N = 17$. The remaining parameters are fixed and have the following values: $t = 1, \mu = 1$ and $\beta = 1$.

All material, except scientific articles or papers published in scientific journals, must, in addition to any notices or disclaimers by the Contractor, also contain the following disclaimer: Any opinions, findings and conclusions or recommendations expressed in this material are those of the author(s) and do not necessarily reflect the views of the Defense Advanced Research Projects Agency (DARPA).

Replace trace by explicit sum $\sum \langle z | \cdot | z \rangle$, then expand the exponent in Taylor series in β

$$\begin{aligned}
 Z &= \sum_z \sum_{n=0}^{\infty} \frac{\beta^n}{n!} \langle z | (-H)^n | z \rangle \\
 &= \sum_z \sum_{n=0}^{\infty} \frac{\beta^n}{n!} \langle z | \left(1 - D_0 - \sum_{j=1} D_j P_j \right)^n | z \rangle \quad (\text{A2}) \\
 &= \sum_z \sum_{n=0}^{\infty} \sum_{\{S_{i_n}\}} \frac{\beta^n}{n!} \langle z | S_{i_n} | z \rangle
 \end{aligned}$$

in last step, $(-H)^n$ expressed in all sequences of length n composed of products of D_0 and $D_j P_j$ which is denoted as $\{S_{i_n}\}$, $\mathbf{i}_n = (i_1, i_2, \dots, i_n)$, $i_j \in \{0, \dots, M\}$ $j \in \{1, \dots, n\}$

$$\begin{aligned}
 Z &= \sum_z \sum_{q=0}^{\infty} \sum_{\{S_q\}} \left(\prod_{j=1}^q d_{z_j}^{(i_j)} \right) \langle z | S_{i_n} | z \rangle \\
 &\quad \left(\sum_{n=q}^{\infty} \frac{\beta^n (-1)^n}{n!} \times \sum_{\sum k_i = n-q} (E_{z_0})^{k_0} \cdots (E_{z_q})^{k_q} \right) \quad (\text{A3})
 \end{aligned}$$

Appendix A: The off-diagonal partition function expansion

Here, we describe the expansion of the partition function in terms of the off-diagonal operators of the Hamiltonian. The partition function is given as:

$$Z = \text{Tr}[e^{-\beta H}] \quad (\text{A1})$$

where $E_{z_i} = \langle z_i | D_0 | z_i \rangle$.

$$d_{z_j}^{(i_j)} = \langle z_j | D_{i_j} | z_j \rangle \quad (\text{A4})$$

$S_{\mathbf{i}_q} = P_{i_q} \dots P_{i_2} P_{i_1}$, $|z_0\rangle = |z\rangle$, $P_{i_j} |z_j\rangle = |z_{j+1}\rangle$. $|z_j\rangle = |z_{(i_1, i_2, \dots, i_j)}\rangle$ $n \rightarrow n + q$ gives:

$$Z = \sum_z \sum_{q=0}^{\infty} \sum_{\{S_q\}} \langle z | S_{\mathbf{i}_q} | z \rangle \left((-\beta)^q \left(\prod_{j=1}^q d_{z_j}^{(i_j)} \right) \times \sum_{n=0}^{\infty} \frac{-\beta^n}{(n+q)!} \sum_{\sum k_i = n} (E_{z_0})^{k_0} \dots (E_{z_q})^{k_q} \right) \quad (\text{A5})$$

$\{E_{z_i}\}$ are classical energies of $|z_i\rangle$ which are created by the application of $S_{\mathbf{i}_q}$.

$$Z = \sum_z \sum_{q=0}^{\infty} \left(\prod_{j=1}^q d_{z_j}^{(i_j)} \right) \sum_{\{S_q\}} \langle z | S_{\mathbf{i}_q} | z \rangle \times \left(\sum_{\{k_i\}=(0, \dots, 0)}^{(\infty, \dots, \infty)} \frac{-\beta^q}{(q + \sum k_i)!} \prod_{j=0}^q (-\beta E_{z_{z_j}})^{k_j} \right) \quad (\text{A6})$$

$$\sum_{\{k_i\}} \frac{-\beta^q}{(q + \sum k_i)!} \prod_{j=0}^q (-\beta E_{z_{z_j}})^{k_j} = e^{-\beta [E_{z_0}, \dots, E_{z_q}]} \quad (\text{A7})$$

$[E_{z_0}, \dots, E_{z_q}]$ is a multiset of energies

$$F[E_{z_0}, \dots, E_{z_q}] \equiv \sum_{j=0}^q \frac{F(E_{z_j})}{\prod_{k \neq j} (E_{z_j} - E_{z_k})} \quad (\text{A8})$$

F is called divided differences, defined for real valued variables $[E_{z_0}, \dots, E_{z_q}]$.

$$Z = \sum_z \sum_{q=0}^{\infty} \sum_{\{S_q\}} \langle z | S_{\mathbf{i}_q} | z \rangle D_{(z, S_{\mathbf{i}_q})} e^{-\beta [E_{z_0}, \dots, E_{z_q}]} \quad (\text{A9})$$

where

$$D_{(z, S_{\mathbf{i}_q})} = \prod_{j=1}^q d_{z_j}^{(i_j)} \quad (\text{A10})$$

Note that, expansion of Z is not an expansion in β . It begins with a Taylor series expansion in β but regrouping of terms into the exponent of divided-differences means no longer a high temperature expansion.

One can interpret Z expansion as a sum of weights. $Z = \sum_{\{\mathcal{C}\}} W_{\mathcal{C}}$, where $\{\mathcal{C}\}$ is all distinct pairs $\{|z\rangle, S_{\mathbf{i}_q}\}$

$$W_{\mathcal{C}} = D_{(z, S_{\mathbf{i}_q})} e^{-\beta [E_{z_0}, \dots, E_{z_q}]} \quad (\text{A11})$$

$W_{\mathcal{C}}$ is the configuration weight. $\langle z | S_{\mathbf{i}_q} | z \rangle$ evaluates to either 1 or 0. Since $P_j, j \neq 0$ has no fixed points, $S_{\mathbf{i}_q} = 1$ implies $S_{\mathbf{i}_q} = \mathbb{1}$. Then,

$$Z = \sum_z \sum_{S_{\mathbf{i}_q} = \mathbb{1}} D_{(z, S_{\mathbf{i}_q})} e^{-\beta [E_{z_0}, \dots, E_{z_q}]} \quad (\text{A12})$$

-
- [1] M. Lewenstein, A. Sanpera, and V. Ahufinger, *Ultracold Atoms in Optical Lattices: Simulating quantum many-body systems* (OUP Oxford, 2012).
- [2] M. P. Fisher, P. B. Weichman, G. Grinstein, and D. S. Fisher, Boson localization and the superfluid-insulator transition, *Physical Review B* **40**, 546 (1989).
- [3] D. Jaksch and P. Zoller, The cold atom hubbard toolbox, *Annals of physics* **315**, 52 (2005).
- [4] T. Giamarchi, C. Rüegg, and O. Tchernyshyov, Bose-einstein condensation in magnetic insulators, *Nature Physics* **4**, 198 (2008).
- [5] G. G. Batrouni, R. T. Scalettar, G. T. Zimanyi, and A. P. Kampf, Supersolids in the bose-hubbard hamiltonian, *Phys. Rev. Lett.* **74**, 2527 (1995).
- [6] F. Hébert, G. G. Batrouni, R. T. Scalettar, G. Schmid, M. Troyer, and A. Dorneich, Quantum phase transitions in the two-dimensional hardcore boson model, *Phys. Rev. B* **65**, 014513 (2001).
- [7] P. Sengupta, L. P. Pryadko, F. Alet, M. Troyer, and G. Schmid, Supersolids versus phase separation in two-dimensional lattice bosons, *Phys. Rev. Lett.* **94**, 207202 (2005).
- [8] D. Heidarian and K. Damle, Persistent supersolid phase of hard-core bosons on the triangular lattice, *Phys. Rev.* Lett. **95**, 127206 (2005).
- [9] S. Wessel and M. Troyer, Supersolid hard-core bosons on the triangular lattice, *Phys. Rev. Lett.* **95**, 127205 (2005).
- [10] M. Boninsegni and N. Prokof'ev, Supersolid phase of hard-core bosons on a triangular lattice, *Phys. Rev. Lett.* **95**, 237204 (2005).
- [11] J.-Y. Gan, Y.-C. Wen, and Y. Yu, Supersolidity and phase diagram of soft-core bosons on a triangular lattice, *Phys. Rev. B* **75**, 094501 (2007).
- [12] B. Bogner, C. De Daniloff, and H. Rieger, Variational Monte-Carlo study of the extended Bose-Hubbard model with short- and infinite-range interactions, *The European Physical Journal B* **92**, 111 (2019).
- [13] W. Krauth, N. Trivedi, and D. Ceperley, Superfluid-insulator transition in disordered boson systems, *Phys. Rev. Lett.* **67**, 2307 (1991).
- [14] W. Krauth and N. Trivedi, Mott and superfluid transitions in a strongly interacting lattice boson system, *EPL (Europhysics Letters)* **14**, 627 (1991).
- [15] J. Kisker and H. Rieger, Bose-glass and mott-insulator phase in the disordered boson hubbard model, *Phys. Rev. B* **55**, R11981 (1997).
- [16] R. G. Melko, A. Parameshwari, A. A. Burkov, A. Vishwanath, D. N. Sheng, and L. Balents, Supersolid order

- from disorder: Hard-core bosons on the triangular lattice, *Phys. Rev. Lett.* **95**, 127207 (2005).
- [17] H. Yokoyama, T. Miyagawa, and M. Ogata, Effect of doublon–holon binding on mott transition–variational monte carlo study of two-dimensional bose hubbard models, *Journal of the Physical Society of Japan* **80**, 084607 (2011), <https://doi.org/10.1143/JPSJ.80.084607>.
- [18] R. T. Scalettar, G. G. Batrouni, and G. T. Zimanyi, Localization in interacting, disordered, bose systems, *Physical review letters* **66**, 3144 (1991).
- [19] P. Sengupta and S. Haas, Quantum glass phases in the disordered bose-hubbard model, *Phys. Rev. Lett.* **99**, 050403 (2007).
- [20] N. Prokof’ev, Revealing Superfluid–Mott–Insulator Transition in an Optical Lattice, in *APS March Meeting Abstracts*, APS Meeting Abstracts, Vol. 2003 (2003) p. H4.002.
- [21] S. Wessel, F. Alet, M. Troyer, and G. G. Batrouni, Quantum monte carlo simulations of confined bosonic atoms in optical lattices, *Physical Review A* **70**, 053615 (2004).
- [22] S. Wessel, F. Alet, S. Trebst, D. Leumann, M. Troyer, and G. George Batrouni, Bosons in optical lattices—from the mott transition to the tonks–girardeau gas, *Journal of the Physical Society of Japan* **74**, 10 (2005).
- [23] L. Pollet, C. Kollath, K. Van Houcke, and M. Troyer, Temperature changes when adiabatically ramping up an optical lattice, *New Journal of Physics* **10**, 065001 (2008).
- [24] J. Y. Gan, Y. C. Wen, J. Ye, T. Li, S.-J. Yang, and Y. Yu, Extended bose-hubbard model on a honeycomb lattice, *Physical Review B* **75**, 214509 (2007).
- [25] K. Kawaki, Y. Kuno, and I. Ichinose, Phase diagrams of the extended bose-hubbard model in one dimension by monte-carlo simulation with the help of a stochastic-series expansion, *Phys. Rev. B* **95**, 195101 (2017).
- [26] A. W. Sandvik, A generalization of Handscomb’s quantum Monte Carlo scheme — Application to the 1-D Hubbard model, *J. Phys. A* **25**, 3667 (1992).
- [27] A. W. Sandvik, Stochastic series expansion method with operator-loop update, *Phys. Rev. B* **59**, R14157 (1999).
- [28] A. W. Sandvik, Ground state projection of quantum spin systems in the valence-bond basis, *Phys. Rev. Lett.* **95**, 207203 (2005).
- [29] A. W. Sandvik and H. G. Evertz, Loop updates for variational and projector quantum monte carlo simulations in the valence-bond basis, *Phys. Rev. B* **82**, 024407 (2010).
- [30] S. V. Isakov, S. Wessel, R. G. Melko, K. Sengupta, and Y. B. Kim, Hard-core bosons on the kagome lattice: Valence-bond solids and their quantum melting, *Phys. Rev. Lett.* **97**, 147202 (2006).
- [31] S. V. Isakov, K. Sengupta, and Y. B. Kim, Bose-hubbard model on a star lattice, *Phys. Rev. B* **80**, 214503 (2009).
- [32] P. Pippal, H. G. Evertz, and M. Hohenadler, Excitation spectra of strongly correlated lattice bosons and polaritons, *Phys. Rev. A* **80**, 033612 (2009).
- [33] R. T. Scalettar, G. G. Batrouni, and G. T. Zimanyi, Localization in interacting, disordered, bose systems, *Phys. Rev. Lett.* **66**, 3144 (1991).
- [34] G. G. Batrouni and R. T. Scalettar, World-line quantum monte carlo algorithm for a one-dimensional bose model, *Phys. Rev. B* **46**, 9051 (1992).
- [35] S. Wessel, F. Alet, S. Trebst, D. Leumann, M. Troyer, and G. George Batrouni, Bosons in optical lattices – from the mott transition to the tonks–girardeau gas, *Journal of the Physical Society of Japan* **74**, 10 (2005), <https://doi.org/10.1143/JPSJS.74S.10>.
- [36] L. Pollet, C. Kollath, K. V. Houcke, and M. Troyer, Temperature changes when adiabatically ramping up an optical lattice, *New Journal of Physics* **10**, 065001 (2008).
- [37] A. van Otterlo and K.-H. Wagenblast, Coexistence of diagonal and off-diagonal long-range order: A monte carlo study, *Phys. Rev. Lett.* **72**, 3598 (1994).
- [38] G. G. Batrouni and R. T. Scalettar, Phase separation in supersolids, *Phys. Rev. Lett.* **84**, 1599 (2000).
- [39] B. Capogrosso-Sansone, S. G. Söyler, N. Prokof’ev, and B. Svistunov, Monte carlo study of the two-dimensional bose-hubbard model, *Phys. Rev. A* **77**, 015602 (2008).
- [40] S. G. Söyler, M. Kiselev, N. V. Prokof’ev, and B. V. Svistunov, Phase diagram of the commensurate two-dimensional disordered bose-hubbard model, *Phys. Rev. Lett.* **107**, 185301 (2011).
- [41] T. Ohgoe, T. Suzuki, and N. Kawashima, Ground-state phase diagram of the two-dimensional extended bose-hubbard model, *Phys. Rev. B* **86**, 054520 (2012).
- [42] B. Capogrosso-Sansone, N. V. Prokof’ev, and B. V. Svistunov, Phase diagram and thermodynamics of the three-dimensional bose-hubbard model, *Phys. Rev. B* **75**, 134302 (2007).
- [43] P. Anders, E. Gull, L. Pollet, M. Troyer, and P. Werner, Dynamical mean field solution of the bose-hubbard model, *Phys. Rev. Lett.* **105**, 096402 (2010).
- [44] Y. Kato and N. Kawashima, Quantum monte carlo method for the bose-hubbard model with harmonic confining potential, *Physical Review E* **79**, 021104 (2009).
- [45] K. Hettiarachchilage, V. G. Rousseau, K.-M. Tam, M. Jarrell, and J. Moreno, Phase diagram of the bose-hubbard model on a ring-shaped lattice with tunable weak links, *Phys. Rev. A* **87**, 051607 (2013).
- [46] L. Gupta, T. Albash, and I. Hen, Permutation matrix representation quantum monte carlo, *Journal of Statistical Mechanics: Theory and Experiment* **2020**, 073105 (2020).
- [47] F. Berger, P. Gritzmann, and S. de Vries, Minimum cycle bases for network graphs, *Algorithmica* **40**, 51 (2004).
- [48] T. Uno and H. Satoh, An efficient algorithm for enumerating chordless cycles and chordless paths, in *Discovery Science*, edited by S. Džeroski, P. Panov, D. Kocev, and L. Todorovski (Springer International Publishing, Cham, 2014) pp. 313–324.
- [49] D. Joyner, *Adventures in Group Theory: Rubik’s Cube, Merlin’s Machine, and Other Mathematical Toys*, Adventures in Group Theory (Johns Hopkins University Press, 2008).
- [50] E. T. Whittaker and G. Robinson, *The calculus of observations: An introduction to numerical analysis* (Dover Publications, 1967).
- [51] C. de Boor, Divided differences, *Surveys in Approximation Theory (SAT)*[electronic only] **1**, 46 (2005).
- [52] E. Akaturk, N. Ezzell, and I. Hen, Permutation matrix representation quantum monte carlo: advanced measurement techniques, (in preparation).
- [53] J. C. dePina, Applications of shortest path methods, (1995).
- [54] T. Kavitha, K. Mehlhorn, D. Michail, and K. E. Paluch, An $\tilde{O}(m^2n)$ algorithm for minimum cycle basis of graphs, *Algorithmica* **52**, 333 (2008).